Robust optimization of the laser induced damage threshold of dielectric mirrors for high power lasers

Marine Chorel, Thomas Lanternier, Eric Lavastre, Nicolas Bonod, Bruno Bousquet, Jérôme Néauport

Research Article | Vol. 26, No. 9 | 30 Apr 2018 | OPTICS EXPRESS 11764
Optics EXPRESS

Robust optimization of the laser induced damage threshold of dielectric mirrors for high power lasers

MARINE CHOREL,[1,*] THOMAS LANTERNIER,[1] ÉRIC LAVASTRE,[1] NICOLAS BONOD,[2] BRUNO BOUSQUET,[3] AND JÉRÔME NÉAUPORT[1]

[1]*Commissariat à l'Energie Atomique et aux Energies Alternatives, Centre d'Etudes Scientifiques et Techniques d'Aquitaine (CEA CESTA), CS60001, 33116 Le Barp Cedex, France*
[2]*Aix Marseille Univ, CNRS, Centrale Marseille, Institut Fresnel, Campus de St Jérôme, 13013 Marseille, France*
[3]*CELIA, Université de Bordeaux UMR5107, 33400 Talence, France*
**marine.chorel@cea.fr*

Abstract: We report on a numerical optimization of the laser induced damage threshold of multi-dielectric high reflection mirrors in the sub-picosecond regime. We highlight the interplay between the electric field distribution, refractive index and intrinsic laser induced damage threshold of the materials on the overall laser induced damage threshold (LIDT) of the multilayer. We describe an optimization method of the multilayer that minimizes the field enhancement in high refractive index materials while preserving a near perfect reflectivity. This method yields a significant improvement of the damage resistance since a maximum increase of 40% can be achieved on the overall LIDT of the multilayer.

OCIS codes: (310.0310) Thin films; (310.6860) Thin films, optical properties; (310.1860) Deposition and fabrication; (310.4165) Multilayer design; (320.0320) Ultrafast optics; (140.3330) Laser damage.

References and links

1. D. Strickland and G. Mourou, "Compression of amplified chirped optical pulses," Opt. Commun. **55**(6), 447–449 (1985).
2. J. D. Zuegel, S. Borneis, C. Barty, B. Legarrec, C. Danson, N. Miyanaga, P. K. Rambo, C. Leblanc, T. J. Kessler, A. W. Schmid, L. J. Waxer, J. H. Kelly, B. Kruschwitz, R. Jungquist, E. Moses, J. Britten, I. Jovanovic, J. Dawson, and N. Blanchot, "Laser challenges for fast ignition," Fus. Sci. Technol. **49**(3), 453–482 (2006).
3. L. Waxer, T. Kessler, D. Maywar, J. Kelly, R. McCrory, B. Kruschwitz, S. Loucks, C. Stoeckl, D. Meyerhofer, and S. Morse, "High-energy petawatt capability for the omega laser," Opt. Photonics News **16**(7), 30–36 (2005).
4. M. Koga, Y. Arikawa, H. Azechi, Y. Fujimoto, S. Fujioka, H. Habara, Y. Hironaka, H. Homma, H. Hosoda, T. Jitsuno, T. Johzaki, J. Kawanaka, R. Kodama, K. Mima, N. Miyanaga, M. Murakami, H. Nagatomo, M. Nakai, Y. Nakata, H. Nakamura, H. Nishimura, T. Norimatsu, Y. Sakawa, N. Sarukura, K. Shigemori, H. Shiraga, T. Shimizu, H. Takabe, M. Tanabe, K. A. Tanaka, T. Tanimoto, T. Tsubakimoto, T. Watari, A. Sunahara, M. Isobe, A. Iwamoto, T. Mito, O. Motojima, T. Ozaki, H. Sakagami, T. Taguchi, Y. Nakao, H. Cai, M. Key, P. Norreys, and J. Pasley, "Present states and future prospect of fast ignition realization experiment (firex) with gekko and lfex lasers at ile," Nucl. Instrum. Methods Phys. Res. A **653**(1), 84–88 (2011).
5. N. Blanchot, G. Béhar, J. C. Chapuis, C. Chappuis, S. Chardavoine, J. F. Charrier, H. Coïc, C. Damiens-Dupont, J. Duthu, P. Garcia, J. P. Goossens, F. Granet, C. Grosset-Grange, P. Guerin, B. Hebrard, L. Hilsz, L. Lamaignere, T. Lacombe, E. Lavastre, T. Longhi, J. Luce, F. Macias, M. Mangeant, E. Mazataud, B. Minou, T. Morgaint, S. Noailles, J. Neauport, P. Patelli, E. Perrot-Minnot, C. Present, B. Remy, C. Rouyer, N. Santacreu, M. Sozet, D. Valla, and F. Laniesse, "1.15 PW-850 j compressed beam demonstration using the PETAL facility," Opt. Express **25**(15), 16957–16970 (2017).
6. N. Blanchot, G. Behar, T. Berthier, B. Busserole, C. Chappuis, C. Damiens-Dupont, P. Garcia, F. Granet, C. Grosset-Grange, J.-P. Goossens, L. Hilsz, F. Laborde, T. Lacombe, F. Laniesse, E. Lavastre, J. Luce, F. Macias, E. Mazataud, J. Miquel, J. Nï, S. Noailles, P. Patelli, E. Perrot-Minot, C. Present, D. Raffestin, B. Remy, C. Rouyer, and D. Valla, Overview of petal, the multi-petawatt project in the lmj facility, **59**, 07001 (2013).
7. A. Casner, T. Caillaud, S. Darbon, A. Duval, I. Thfouin, J. Jadaud, J. LeBreton, C. Reverdin, B. Rosse, R. Rosch, N. Blanchot, B. Villette, R. Wrobel, and J. Miquel, "Lmj/petal laser facility: Overview and opportunities for laboratory astrophysics," High Energy Density Physics **17**, 2–11 (2015).
8. M. Mero, J. Liu, W. Rudolph, D. Ristau, and K. Starke, "Scaling laws of femtosecond laser pulse induced breakdown in oxide films," Phys. Rev. B **71**(11), 115109 (2005).

#322955 https://doi.org/10.1364/OE.26.011764
Journal © 2018 Received 9 Feb 2018; revised 21 Mar 2018; accepted 22 Mar 2018; published 23 Apr 2018

Optics EXPRESS

9. B. Mangote, L. Gallais, M. Commandré, M. Mende, L. Jensen, H. Ehlers, M. Jupé, D. Ristau, A. Melninkaitis, J. Mirauskas, V. Sirutkaitis, S. Kičas, T. Tolenis, and R. Drazdys, "Femtosecond laser damage resistance of oxide and mixture oxide optical coatings," Opt. Lett. **37**(9), 1478–1480 (2012).
10. L. Gallais and M. Commandré, "Laser-induced damage thresholds of bulk and coating optical materials at 1030 nm, 500 fs," Appl. Opt. **53**(4), A186–A196 (2014).
11. A. Hervy, L. Gallais, G. Cheriaux, and D. Mouricaud, "Femtosecond laser-induced damage threshold of electron beam deposited dielectrics for 1-m class optics," Opt. Eng. **56**(1), 011001 (2017).
12. J. B. Oliver, P. Kupinski, A. L. Rigatti, A. W. Schmid, J. C. Lambropoulos, S. Papernov, A. Kozlov, C. Smith, and R. D. Hand, "Stress compensation in hafnia/silica optical coatings by inclusion of alumina layers," Opt. Express **20**(15), 16596–16610 (2012).
13. J. Bellum, E. Field, D. Kletecka, and F. Long, "Reactive ion-assisted deposition of e-beam evaporated titanium for high refractive index tio2 layers and laser damage resistant, broad bandwidth, high-reflection coatings," Appl. Opt. **53**(4), A205–A211 (2014).
14. M. Jupe, M. Lappschies, L. Jensen, K. Starke, and D. Ristau, "Improvement in laser irradiation resistance of fs-dielectric optics using silica mixtures," in *Laser-Induced Damage in Optical Materials*: 2006, vol. 6403, G. J. Exarhos, A. H. Guenther, K. L. Lewis, D. Ristau, M. J. Soileau, and C. J. Stolz, eds. (SPIE, 2006), vol. 6403, p. 64031A.
15. L. O. Jensen, M. Mende, H. Blaschke, D. Ristau, D. Nguyen, L. Emmert, and W. Rudolph, Investigation on SiO2/HfO2 mixtures for nanosecond and femtosecond pulses, in Laser-Induced Damage in Optical Materials, vol. 7842, G. J. Exarhos, V. E. Gruzdev, J. A. Menapace, D. Ristau, and M. J. Soileau, eds. (SPIE, 2010), vol. 7842, p. 784207.
16. A. Melninkaitis, T. Tolenis, L. Mažulė, J. Mirauskas, V. Sirutkaitis, B. Mangote, X. Fu, M. Zerrad, L. Gallais, M. Commandré, S. Kičas, and R. Drazdys, "Characterization of zirconia- and niobia-silica mixture coatings produced by ion-beam sputtering," Appl. Opt. **50**(9), C188–C196 (2011).
17. M. Mende, S. Schrameyer, H. Ehlers, D. Ristau, and L. Gallais, "Laser damage resistance of ion-beam sputtered Sc2o3/Sio2 mixture optical coatings," Appl. Opt. **52**(7), 1368–1376 (2013).
18. T. Willemsen, M. Jupé, M. Gyamfi, S. Schlichting, and D. Ristau, "Enhancement of the damage resistance of ultra-fast optics by novel design approaches," Opt. Express **25**(25), 31948–31959 (2017).
19. L. M. Stolz, C. J. Sheehan, M. K. Von Gunten, R. P. Bevis, and D. J. Smith, "The advantages of evaporation of hafnium in a reactive environment to manufacture high damage threshold multilayer coatings by electron-beam deposition, in European Optical Society Symposium on Optical system design and production," Proc. SPIE **3738**, 318–324 (1999).
20. J. B. Oliver and D. Talbot, "Optimization of deposition uniformity for large-aperture national ignition facility substrates in a planetary rotation system," Appl. Opt. **45**(13), 3097–3105 (2006).
21. J. H. Apfel, "Optical coating design with reduced electric field intensity," Appl. Opt. **16**(7), 1880–1885 (1977).
22. D. Schiltz, D. Patel, L. Emmert, C. Baumgarten, B. Reagan, W. Rudolph, J. J. Rocca, and C. S. Menoni, "Modification of multilayer mirror top-layer design for increased laser damage resistance," Proc. SPIE **9237**, 92371G (2014).
23. G. Abromavicius, R. Buzelis, R. Drazdys, A. Melninkaitis, and V. Sirutkaitis, "Influence of electric field distribution on laser induced damage threshold and morphology of high reflectance optical coatings," Proc. SPIE **6720**, 67200Y (2007).
24. S. Chen, Y. Zhao, Z. Yu, Z. Fang, D. Li, H. He, and J. Shao, "Femtosecond laser-induced damage of Hfo2/Sio2 mirror with different stack structure," Appl. Opt. **51**(25), 6188–6195 (2012).
25. H. Becker, D. Tonova, M. Sundermann, L. Jensen, M. Gyamfi, D. Ristau, and M. Mende, "Advanced femtosecond laser coatings raise damage thresholds," Proc. SPIE **9627**, 962716 (2015).
26. D. Patel, D. Schiltz, P. F. Langton, L. Emmert, L. N. Acquaroli, C. Baumgarten, B. Reagan, J. J. Rocca, W. Rudolph, A. Markosyan, R. R. Route, M. Fejer, and C. S. Menoni, "Improvements in the laser damage behavior of Ta2O5/SiO2 interference coatings by modification of the top layer design," Proc. SPIE **8885**, 888522 (2013).
27. A. L. Bloom and V. R. Costich, "5.5 design for high power resistance," in *Laser Induced Damage in Optical Materials, 1975* (1976).
28. S. Chen, Y. Zhao, H. He, and J. Shao, "Ef fect of standing-wave f ield distribution on femosecond laser-induced damage of HfO2/SiO2 mirror coating," Chin. Opt. Lett. **9**(8), 083101 (2011).
29. F. Demichelis, E. Mezzetti-Minetti, L. Tallone, and E. Tresso, "Optimization of optical parameters and electric field distribution in multilayers," Appl. Opt. **23**(1), 165–171 (1984).
30. A. V. Tikhonravov, M. K. Trubetskov, and G. W. Debell, "Application of the needle optimization technique to the design of optical coatings," Appl. Opt. **35**(28), 5493–5508 (1996).
31. A. V. Tikhonravov, M. K. Trubetskov, and G. W. DeBell, "Optical coating design approaches based on the needle optimization technique," Appl. Opt. **46**(5), 704–710 (2007).
32. A. V. Tikhonravov and M. K. Trubetskov, *OptiLayer Thin Film Software Manual*, OptiLayer GmbH (2015).
33. I. B. Angelov, M. von Pechmann, M. K. Trubetskov, F. Krausz, and V. Pervak, "Optical breakdown of multilayer thin-films induced by ultrashort pulses at MHz repetition rates," Opt. Express **21**(25), 31453–31461 (2013).
34. K. Ohta and H. Ishida, "Matrix formalism for calculation of electric field intensity of light in stratified multilayered films," Appl. Opt. **29**(13), 1952–1959 (1990).

Optics EXPRESS

35. J. B. Oliver, "Impact of deposition-rate fluctuations on thin-film thickness and uniformity," Opt. Lett. **41**(22), 5182–5185 (2016).

1. Introduction

The chirped pulse amplification technique proposed in 1985 by Strickland and Mourou [1] has allowed for the development of Petawatt class laser systems [2] such as OMEGA EP [3], FIREX [4] and PETAL [5–7]. However, the overall performance of high power laser facilities is currently limited by the damage resistance of optical components, especially mirrors placed after the compression stage of the chirped pulse amplifier. Increasing the Laser Induced Damage Threshold (LIDT) of multilayer mirrors is therefore of crucial importance to increase the laser power of Petawatt class systems.

LIDT is governed in the short-pulse regime (*i.e.* picosecond to sub-picosecond) by electronic processes. The LIDT of a multilayer stack depends on the Electric Field Intensity (EFI) distribution inside the layers and on the intrinsic physical property of the materials, named hereafter as "intrinsic LIDT". It has been shown that there is a linear relationship between the intrinsic LIDT and the optical bandgap energy of the material [8–11]. Consequently, we can distinguish two complementary trends in the enhancement of damage performance of dielectric mirrors in short pulse regime: optimizing materials to improve damage resistance and/or work on stack design to adapt electric field. Materials used for building multilayer mirrors for high power ultrashort applications are typically the same as those developed in the context of nanosecond high threshold coatings, mainly oxides and fluorides [8, 10, 12, 13]. Significant progresses were also obtained by using mixtures of dielectrics to improve band-gap and thus damage resistance [9, 14–16, 17]. More recently, nano-laminates brought another step forward in the engineering of material band gap [18]. Despite this large choice of materials, HfO_2 and SiO_2 are still materials that are the most widely used for high performance large size optical coatings [19, 20].

Considerable work has also been reported on the engineering of the electric field intensity on the multilayer coating. On binary mirror stacks, Apfel modified the upper layers to reduce the electric field intensity in the high index material [21, 22]. This approach, also extended to a higher number of layers (also called reduced standing wave design), was proved to improve the LIDT in the short pulse regime [13, 23-25]. Ternary mirror designs were also proposed with the idea of using HfO_2 only where high electric field intensities could not be avoided, and a higher index material (albeit less damage resistant) elsewhere to reduce the number of pairs necessary to attain the desired reflectivity [26]. Interestingly enough, authors studied the role of interface on stress [27]. Based on these results, specific designs were proposed to reduce the electric field at interfaces to improve damage resistance with contradictory experimental results, probably due to a lack of robustness of the designs [28].

Here we propose to use an optimization algorithm to determine the optimal design of binary mirrors given a set of materials characterized by their index of refraction and intrinsic damage resistance. For this purpose, [13, 21] optimization algorithms such as the gradient optimization proposed by Demichelis *et al.* [29] or the needle optimization [30, 31] provided for example in Optilayer software [32] can be used. Those algorithms operate by minimizing a merit function, taking into account the different, sometimes conflicting goals, such as minimum reflectivity, group delay dispersion, spectral width, electric field, etc. The difficulty is to find the global minimum and to avoid local minima. In what follows, we propose a systematic approach to find an optimal material choice in the case of binary mirror stacks. We numerically show how to increase the LIDT of multilayer mirrors (*i*) by evaluating designs with alternative materials to the conventional HfO_2/SiO_2 couple and (*ii*) by investigating designs using those materials deviated from quarter wavelength optical thickness layers. Dielectric materials are ranked after a parametric study on the EFI and LIDT. Lack of robustness in a design can lead to performance being not as good as expected [28, 33], we then present a method to obtain a "global optimum" design taking into account reflectivity,

Optics EXPRESS

LIDT and robustness to manufacturing variations and to uncertainties on the physical parameters of the materials. This work has been carried out in the framework of the PETAL laser facility but the method reported here is general and can be applied to other facilities.

2. Quarter wavelength mirror

2.1 Distribution of electric field intensity

The Petal transport mirrors are exposed to 700-fs laser pulses at a 45° incidence angle. Their reflectivity must be higher than 99% for either *p* or *s* polarization at 1053 nm, the central wavelength of the laser radiation.

This study deals with designs consisting of alternating layers of two materials, one of which has a high refractive index and the other a low refractive index. The first and last layers have a high refractive index. We consider a reference design consisting of 31 layers, each layer having an optical thickness of one quarter wavelength (QWOT) at the design wavelength and incidence angle. This number of layers ensures a reflectivity near 100% for both *p* and *s* polarizations. The distribution of the EFI in this design is presented in Fig. 1 with hafnia and silica as high and low refractive index materials, respectively.

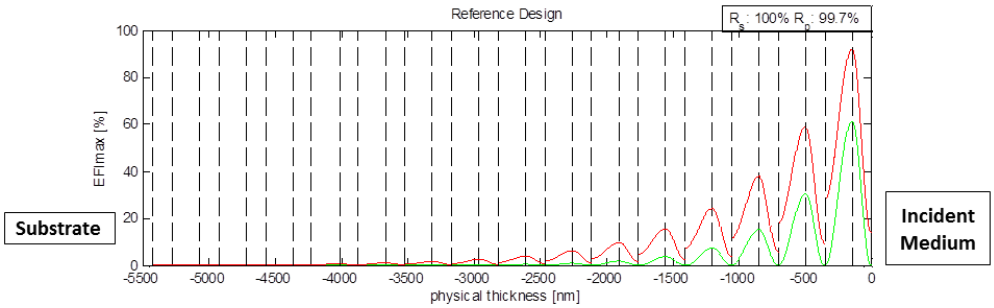

Fig. 1. Electric Field Intensity distribution for s (green) and p (red) polarization in a $(HL)^{15}H$ stack where H is HfO_2 and L is SiO_2. The incident medium, air, is located on the right of the stack and the substrate on the left. The electric field distribution is expressed as a percentage of the incident electric field intensity.

Let us notice that (*i*) we did not take into account the group delay dispersion because of the narrow bandwidth (about 5nm) and (*ii*) we considered stacks made of two materials and not with three or more materials. Such designs with three materials are often used for mechanical reasons [12] and not especially for improving laser damage resistance.

In this study, all the calculations are performed with MATLAB using the matrix formalism detailed in [34]. The results are also verified with the commercial software Optilayer.

2.2 Laser induced damage threshold of high and low refractive index materials

We review in Table 1 the different dielectric materials available for physical vapor deposition, their refractive index, intrinsic LIDT and bandgap energy taken in [10].

Optics EXPRESS

Table 1. Optical Constants of Material Thin Films (from [10] [10] otherwise specified)

	Material	Refractive index (at 1030nm)	Bandgap (eV)	Intrinsic LIDT (J/cm^2)	Deposition method
Low refractive index materials (L)	SiO_2	1.46	7.49	3.15 ± 0.35	E-Beam Deposition
	MgF_2	1.35	unknown	2.66 ± 0.07	not specified
High refractive index materials (H)	Al_2O_3	1.65	6.46	2.52 ± 0.16	not specified
	$Sc_2O_{3\,a}$	1.9	5.6	2.1 ± 0.02	
	$Sc_2O_{3\,b}$ [17]		5.7	3.1	
	$HfO_{2\,a}$	1.94	5.31	1.78 ± 0.07	E-Beam Deposition
	Ta_2O_5	2.09	4.10	1.05 ± 0.04	Dual Ion Beam Sputtering
	ZrO_2	2.09	4.74	1.66 ± 0.02	E-Beam Deposition
	TiO_2	2.29	3.6	0.77 ± 0.08	E-Beam Deposition

If we rank the low refractive index materials according to their intrinsic LIDT, SiO_2 comes first followed by MgF_2. Concerning high refractive index materials, Al_2O_3 can be considered as the best candidate. As we can see in Table 1, materials characterized by the highest intrinsic LIDT often have a low refractive index. However, the LIDT of the mirror also depends on the maximum of the EFI which in turn depends on the thickness and the refractive index of each layer. Let us first study the impact of the refractive index on the maximum of the EFI (EFI_{max}).

2.3 Influence of material index on the maximum of electric field intensity

The EFI is calculated in the reference design when varying the values of the low and high refractive index from 1.3 to 1.55 and from 1.65 to 2.2 respectively. The calculated EFI_{max} values are displayed in Fig. 2 as a function of the high refractive index (horizontal axis) and low refractive index (vertical axis) for both *p* (left) and *s* (right) polarizations. The coordinates of a few pairs of high / low refractive index materials are superimposed to the density plot of EFI. Figure 2 reveals that for this type of design, EFI_{max} is mainly influenced by the high refractive index as the colors form mostly vertical lines. We can also remark that the highest values of the high refractive index provide the lowest values of EFI_{max}.

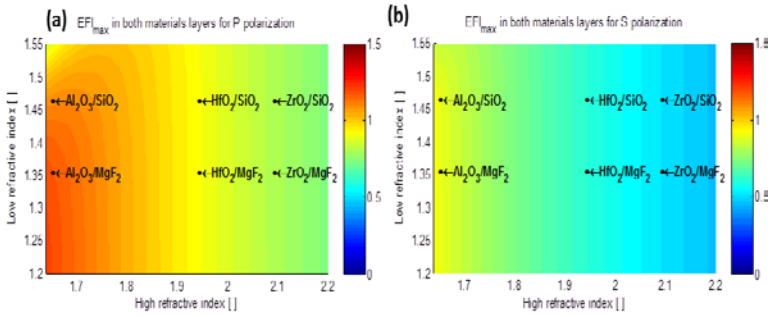

Fig. 2. Maximum of the Electric Field Intensity (EFI_{max}) calculated in the reference stack composed of two materials under the design $(HL)^{15}H$ for the *p* (a) and the *s* polarization (b) as a function of the high (x axis) and low (y axis) refractive index. Only a few materials are represented to facilitate reading.

Two pairs of materials to build multilayer mirrors with reduced EFI, namely ZrO_2/SiO_2 and ZrO_2/MgF_2 appear as good candidates. At the opposite, one can also conclude that the pairs Al_2O_3/SiO_2 and Al_2O_3/MgF_2 correspond to the highest EFI_{max}. Let us point out that

Optics EXPRESS

based on the intrinsic LIDT values given in Table 1 only, Al_2O_3 should be selected among the list of high refractive index materials. This difference between the results provided by Table 1 (LIDT) and Fig. 2 (EFI) highlights the fact that the whole stack of layers must be considered instead of individual layers separately. Nevertheless the LIDT of the entire mirror depends not only on the EFI_{max} but also on the intrinsic LIDT of each layer.

2.4 Laser induced damage threshold (LIDT) of the multilayer mirror

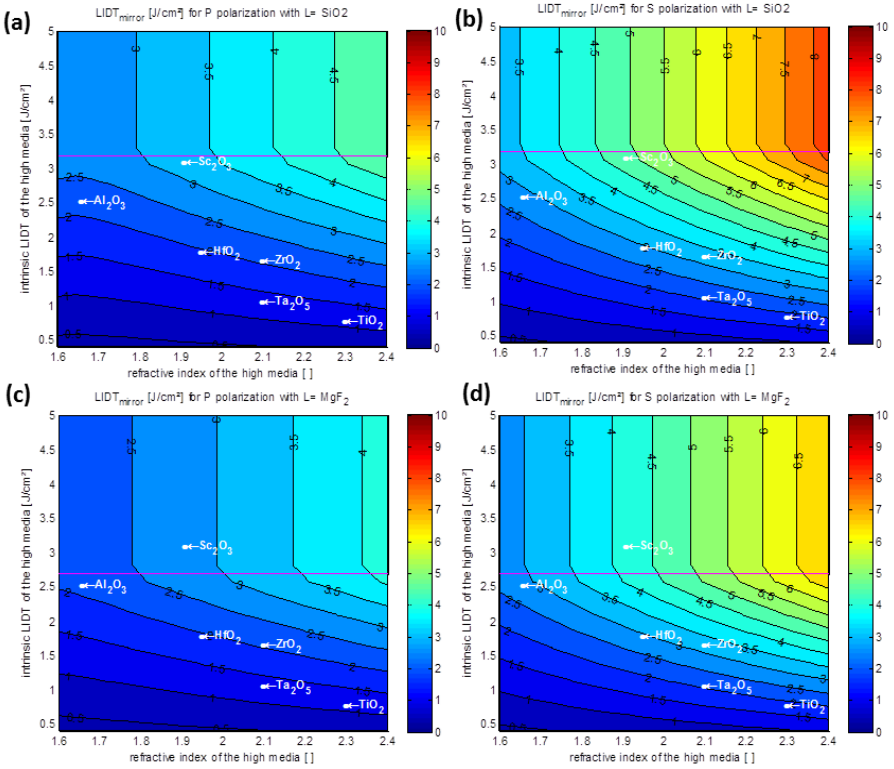

Fig. 3. LIDT of the reference multilayer mirror (colors) as a function of high refractive index values (*x* axis) and intrinsic LIDT values of the high refractive index materials (*y* axis) for the *p* (left) and *s* (right) polarizations. The low refractive index is fused silica (upper two figures, a and b) and magnesium fluoride (the two bottom figures, c and d). The purple line delimitates the region where the damage occurs: under (over) this line it is the high (low) refractive index materials.

The objective of this section is to select the high refractive index materials of the reference design by calculating the LIDT value of the entire mirror as a function of both the high refractive index n_H and the intrinsic LIDT of the high index material denoted $LIDT_{int,H}$. In this calculation, the low index parameters are fixed since it was showed in Fig. 2 that the influence of the low refractive index on the EFI_{max} is limited. However we did the calculation for two different low refractive index materials: SiO_2 and MgF_2.

In a first step, the values of the high refractive index n_H are varied from 1.6 to 2.4 while the values of the intrinsic LIDT are varied from 0.5J/cm^2 to 5J/cm^2 in order to take into account all the materials presented in Table 1. In a second step, the EFI is calculated in the multilayer and the two maxima $EFI_{max,H}$ and $EFI_{max,L}$ in the high and low refractive index materials respectively are recorded. In a third step, the LIDT of the high and low refractive index materials denoted respectively $LIDT_H$ and $LIDT_L$ are evaluated by calculating the ratio between the intrinsic LIDT of the material and EFI_{max} in this same material: $LIDT_H = LIDT_{int,H}/EFI_{max,H}$, $LIDT_L = LIDT_{int,L}/EFI_{max,L}$ [10, 17]. The LIDT of the entire multilayer is

Optics EXPRESS

taken equal to the minimum value between $LIDT_L$ and $LIDT_H$ and is displayed in Fig. 3 as a density plot. The purple line separates the regions where the damage occurs in the low refractive index material (above, $LIDT_L<LIDT_H$) and the high refractive index material (below, $LIDT_L>LIDT_H$).

Figure 3 shows that LIDT values obtained with this method are significantly different for the two states of polarization. For example, with HfO_2 and SiO_2, the LIDT performance is 1.93J/cm^2 for the *p* polarization and 2.90J/cm^2 for the *s* polarization. Thus, it might be helpful to specifically design a multilayer mirror depending on the polarization. However, the values of LIDT for the entire mirror evolve in roughly the same way according to the two states of polarization.

We can also note from Fig. 3 that two materials such as Al_2O_3 and ZrO_2 characterized by very different values of refractive index (1.65 and 2.09 respectively) and intrinsic LIDT (2.52J/cm^2 and 1.66J/cm^2 respectively) provide multilayer mirrors (based on fused silica as the low refractive index material) characterized by similar values of LIDT. Let us point out that these two materials were considered in Table 1 as the best and almost the worst candidates (considering only the intrinsic LIDT values) and in Fig. 2 as the worst and almost best candidates (considering the EFI_{max} in the reference stack).

Based on the results displayed in Fig. 3, Sc_2O_3 features the highest LIDT values for the entire mirror, namely 3.25J/cm^2 for the *p* polarization (left) and 4.82J/cm^2 for the *s* polarization (right). Sc_2O_3 consequently represents the best compromise between the value of the high refractive index and those of the intrinsic LIDT. Finally, based on Fig. 3, it is possible to compare the high refractive index materials through their influence on the general LIDT of silica-based multilayer mirrors of the same architecture.

2.5 Optimization of the two outer layers

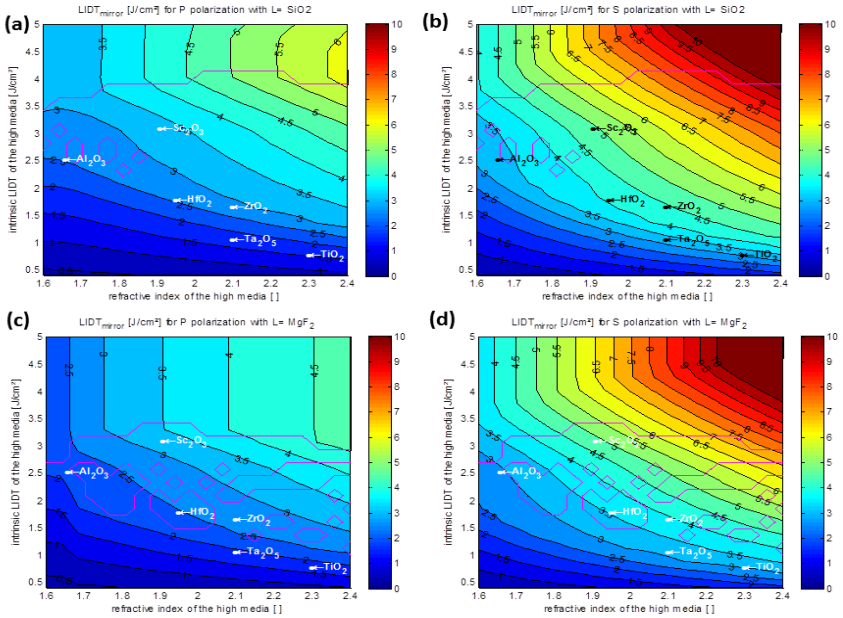

Fig. 4. LIDT of multilayer mirrors, the reference design with the two outer layer thicknesses optimized, (colors) as functions of high refractive index values (*x* axis) and intrinsic LIDT values of the high refractive index materials (*y* axis) for the *p* (left) and the *s* (right) polarizations. The low refractive index is fused silica (upper two figures, a and b) and magnesium fluoride (the two bottom figures, c and d). The purple line delimitates the region where the damage occurs: under (over) this line it is the high (low) refractive index materials.

Optics EXPRESS

Figure 1 reveals that the two outer layers of a mirror are exposed to the highest EFI. We can thus optimize their thickness to improve the LIDT of the entire mirror as proposed by Apfel *et al.* [21] by shifting the EFI peak inside the material characterized by the highest intrinsic LIDT value. We applied this optimization method to the previous calculation and obtained the results displayed in Fig. 4.

This optimization does not change the ranking of the materials but increases all the LIDT performances. For the HfO_2/SiO_2 pair, the overall LIDT is increased by 31% for the *p* polarization and by 33% for the *s* polarization. With this optimization, the high refractive index layer thickness is reduced and the low refractive index layer thickness is increased. This result will be confirmed later in Fig. 5 when optimizing the 12 upper layers.

The LIDT values presented in this section were based on the reference design composed of QWOT layers except the two outer layers which have optimized thicknesses to enhance the LIDT value. Even if these types of QWOT-based designs are widely used, other combinations of layers might exhibit higher LIDT values and this question is addressed in the next section.

3. Optimization of multilayer stacks

The objective now is to define new designs for the *p* polarization by generating layer thicknesses randomly. The random generation covers most of the design possibilities and permits to determine interesting designs completely different from the initial reference design.

Here, we consider the reference design with HfO_2 and SiO_2 using refractive index and intrinsic LIDT in Table 1. Since the outer layers of a mirror are exposed to the highest EFI (see Fig. 1), we modified only the thicknesses of the 12 outer layers. The 19 inner layers guaranteed reflectivity values of >99% for the *s* polarization and >95% for the *p* polarization.

Regarding the range of thickness, the minimal value should be realistic regarding the thinnest layer that can be achieved by the deposition process. Based on technical considerations, this minimum value was set to 20 nm. As the EFI varies periodically inside a layer with a period of half-wave optical thickness, the range of variation needs to be equal (or wider) to a half-wave optical thickness. So the maximum thickness was set to 500nm for both materials which corresponds to almost 3.5 QWOT for a high index layer and less than 2.5 QWOT for a low index layer.

The first step of the calculation corresponds to the generation of a multitude of designs with random thicknesses uniformly distributed between the minimum and the maximum thicknesses. We generated randomly around 9 million designs. The second step is to filter the solutions satisfying conditions on reflectivity (>99% at 1053nm) and LIDT (> 2J/cm^2) for the *p* polarization. Applying these criteria, the number of solutions was reduced by 99.93% (6067 solutions). The third and last step consisted in evaluating the robustness of the remaining solutions regarding thickness variations, refractive index variations and also intrinsic LIDT of both material variations.

To test the robustness regarding thickness variations, we first modified the thickness of the 12 layers of ± 3 nm for each of the 6067 designs. This error corresponds to a modification of around 3% of the thicker quarter wave optical thickness [35]. Solutions are selected regarding the reflectivity and LIDT. We applied the same approach routine to test the robustness for refractive index variations and intrinsic LIDT variations. With a variation of refractive index of ± 0.03, we consider to overestimate the real index variations which include the index variation induced by the porosity of the coating and the measurement variations.

Let us remember that the intrinsic LIDT is defined as the product of the EFI_{max} and the experimental LIDT ($LIDT_{int,i} = EFI_{max,i} . LIDT_i$ with i = L,H) . Errors on the EFI_{max} have already been evaluated with the errors on thickness and refractive index. Regarding the errors on the experimental LIDT, we consider that we are able to determine the intrinsic LIDT with a 5% precision leading to a variation of LIDT of ± 0.08J/cm^2 in this test.

Optics EXPRESS

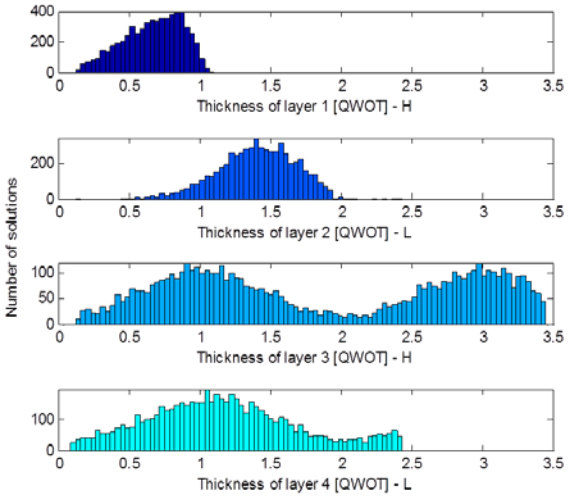

Fig. 5. Distribution of the 6067 solutions (satisfying criteria: reflectivity > 99%, LIDT > 2J/cm^2) as a function of layer thickness normalized to QWOT for the 4 outer layers. Layer 1 corresponds to the outer layer and the thickness is given in units of QWOT.

The distributions of the screened solutions are displayed in Fig. 5 with respect to the thickness of the 4 outer optical layers. The number of solutions is clearly higher for thickness of layers 3 and 4 close to the QWOT (high reflectivity). It is interesting to mention that the other layers (from layer 5 to layer 12) exhibited the same histograms as layers 3 and 4. For the first layer, most of the solutions correspond to thicknesses lower than one QWOT, with a maximum of the histogram around 0.8 QWOT. For the second layer, the largest number of solutions is obtained around 1.4 QWOT. From these results, we can conclude that the final design should exhibit a thin high index material outer layer (the least resistant material to laser induced damage) and a thicker low index material layer (the most resistant). This conclusion is in good agreement with the results reported by Apfel *et al.* [21] The first and second robustness tests on thickness and refractive index drastically decreases the number of solutions to only 84. This value stays unchanged after applying the test of robustness related to the variations of intrinsic LIDT, which was expected since the variations of intrinsic LIDT were already *via* the variations of thickness and refractive index.

Finally, these 84 different mirror designs exhibit higher reflectivity than the minimal reflectivity 99% and higher LIDT than the reference design. Among this set of 84 solutions compatible with manufacturing errors, the solution exhibiting the highest LIDT is characterized by an LIDT value of 2.73 J/cm^2 and a reflectivity value of 99.37% for the *p* polarization. The thicknesses of the 12 outer layers of this design are reported in Table 3. Let us emphasize that this value of LIDT is 41% higher than that of the reference design (1.93J/cm^2) and 9% better than that of a mirror with only the two outer layers optimized (2.54J/cm^2, see Fig. 4).

All the results presented until now have been obtained after considering the manufacturing errors separately on each factor. To go further into this study, let us now apply the effect of possible cumulative errors on the set of 84 solutions presented above. We thus simultaneously reduce all the thicknesses by 3nm, refractive index by 0.03 and intrinsic LIDT by 0.08 J/cm^2 as it corresponds to the worst possible case. With this cumulative error, there are only 2 designs with a reflectivity higher than 99% and LIDT higher than 2 J/cm^2. The best solution exhibited an LIDT value of 2.08J/cm^2 with the cumulative errors and an LIDT value of 2.22J/cm^2 considering the nominal values of thickness, refractive index and intrinsic LIDT. The thicknesses of the 12 outer layers of this design are reported in Table 3. In our previous calculation considering the manufacturing errors step by step, the best solution exhibited an

Optics EXPRESS

LIDT value of 2.73J/cm^2. This value dropped to 1.75J/cm^2 when considering potential cumulative errors. Note also that when applying the approach of cumulative errors to our reference design, the LIDT value felt from 1.93J/cm^2 to 1.71J/cm^2. Finally, the LIDT values of the design with the two outer layers optimized dropped from 2.54J/cm^2 to 1.89J/cm^2. Table 2 summarizes these results.

Table 2. Best LIDT performance and related designs

	LIDT under nominal conditions [J/cm^2]	LIDT under cumulative errors [J/cm^2]
Reference QWOT design	1.93	1.71
Design optimized as function of the 2 outer layers	2.54	1.89
Design optimized as function of the 12 outer layers	2.73	1.75
Design optimized as function of the 12 outer layers featuring the highest LIDT with cumulative errors	2.22	2.08

The design corresponding to the last row in Table 2 corresponds to the solution with the highest LIDT assuming cumulative errors. Figure 6 exhibits the EFI across the corresponding stack with and without the cumulative errors. It reveals that in the nominal conditions the damage occurs in layer 3. With the cumulative errors, the damage will occur at the interface between layers 1 and 2. So the most stable design will not always damage at the interface between the two outer layers.

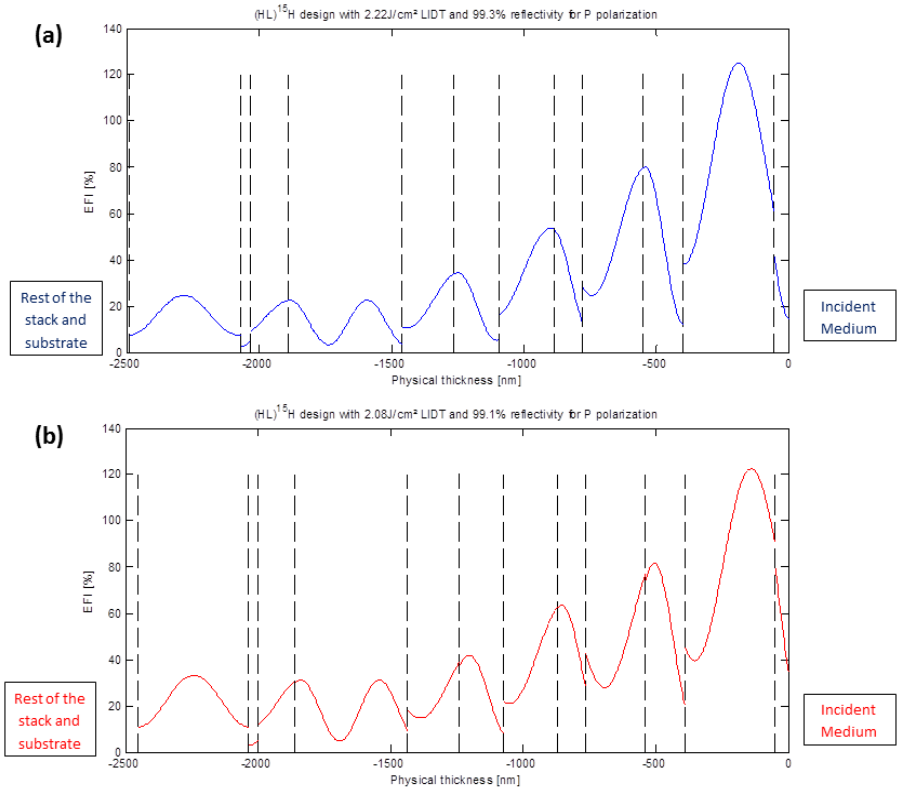

Fig. 6. EFI distribution for *p* polarization in the 12 outer layers of the more stable design in nominal conditions (blue) LIDT = 2.22J/cm^2 and with cumulative errors on the thicknesses, index and intrinsic LIDT (red) LIDT = 2.08J/cm^2

Optics EXPRESS

Table 3. Thickness of layers of the best designs

	Physical thickness [nm] of layers											
	12	11	10	9	8	7	6	5	4	3	2	1
Design optimized as function of the 12 outer layers	218	108	213	228	434	475	289	156	208	108	313	89
Design optimized as function of the 12 outer layers featuring the highest LIDT with cumulative errors	420	40	141	428	198	169	207	109	230	151	342	54

4. Conclusion

We performed a numerical investigation of the laser damage resistance of high reflection mirror stacks using two dielectric materials. This study was carried out by calculating the electric field distribution in the stack using values of refractive index and material damage resistance (intrinsic laser-induced damage threshold, LIDT) from the literature. We evidenced that damage resistance of materials has to be compared in a complete stack. A selection of materials based on their intrinsic LIDT only was demonstrated to be insufficient to predict the optimum mirror. A modification of the two outer layers of a QWOT stack gives rise to an increase in damage resistance which depends on the pair of materials retained. But the material ranking using a QWOT design is not changed. An optimization of a full stack was also performed. This optimization brings limited improvement of damage resistance but can bring solutions which are more resistant to manufacturing errors. This theoretical approach will be applied for the manufacturing of mirror stacks that will be measured in terms of reflectivity and damage.